Editors' Suggestion Featured in Physics

Evidence for a Spatially Modulated Superfluid Phase of ^{3}He under Confinement

Lev V. Levitin,* Ben Yager,† Laura Sumner,‡ Brian Cowan, Andrew J. Casey, and John Saunders
Department of Physics, Royal Holloway University of London, Egham, Surrey TW20 0EX, United Kingdom

Nikolay Zhelev,§ Robert G. Bennett,∥ and Jeevak M. Parpia
Department of Physics, Cornell University, Ithaca, New York 14853, USA

(Received 8 May 2018; revised manuscript received 12 December 2018; published 27 February 2019)

In superfluid ^{3}He-B confined in a slab geometry, domain walls between regions of different order parameter orientation are predicted to be energetically stable. Formation of the spatially modulated superfluid *stripe phase* has been proposed. We confined ^{3}He in a 1.1 μm high microfluidic cavity and cooled it into the B phase at low pressure, where the stripe phase is predicted. We measured the surface-induced order parameter distortion with NMR, sensitive to the formation of domains. The results rule out the stripe phase, but are consistent with 2D modulated superfluid order.

DOI: 10.1103/PhysRevLett.122.085301

The pairing of fermions to form a superfluid or superconductor at sufficiently low temperatures is a relatively ubiquitous phenomenon [1,2]. Examples include electrically conducting systems from metals to organic materials to metallic oxides [3], neutral atoms from ^{3}He [4,5] to ultracold fermionic gases [6], and astrophysical objects such as neutron stars and pulsars [7]. In the most straightforward case the pairs form a macroscopic quantum condensate which is spatially uniform. In type-II superconductors a spatially inhomogeneous state, the Abrikosov flux lattice, arises in a magnetic field [8]. Its origin is the negative surface energy between normal and superconducting regions. However, the realization and experimental identification of states with spatially modulated superfluid or superconducting order has proved challenging.

The Fulde-Ferrell-Larkin-Ovchinnikov (FFLO) state [9,10], has been predicted to arise in *spin-singlet* superconductors. An imbalance between spin-up and spin-down Fermi momenta, driven by ferromagnetic interactions or high magnetic fields, induces pairing with nonzero center of mass momentum. This results in both the order parameter and the spin density oscillating in space with the same wave vector. The FFLO state is predicted to intervene beyond the Pauli limiting field, inhibiting the destruction of superconductivity [11]. It requires orbital effects to be weak, restricting possible materials for its observation. There is evidence of the FFLO state in the layered organic superconductors κ-(BEDT-TTF)$_2$Cu(NCS)$_2$ and β''-(ET)$_2$SF$_5$CH$_2$CF$_2$SO$_3$ [12–16], and in the canonical heavy fermion superconductor CeCu$_2$Si$_2$ [17]. Previously identified as the FFLO state [18], a more complex state, with intertwined p-wave pair density wave (PDW) and spin density wave has been proposed in the heavy fermion d-wave superconductor CeCoIn$_5$ [19–21]. Elsewhere a PDW commensurate with a charge density wave has been clearly demonstrated in the d-wave cuprate superconductor Bi$_2$Sr$_2$CaCu$_2$O$_{8+x}$ [22]. In the ultracold fermionic gas ^{6}Li, superfluidity with imbalanced spin populations has been observed [23] with thermodynamic evidence consistent with the FFLO state [24]. In addition to these condensed matter systems, it has been proposed that quantum chromodynamics may provide a pathway to inhomogeneous superconductivity, potentially realized in astrophysical objects [25].

In general the order parameter modulation is expected to be more complex than the model FFLO state [11,26]. Potential examples are 1D domain walls of thickness much smaller than the width of domains, and 2D modulated structures, involving multiple wave vectors [11]. Furthermore, nucleation barriers and metastability may inhibit the formation of periodic states [26].

In this Letter we report experimental investigation of a predicted spatially modulated state in the topological p-wave, *spin-triplet*, superfluid ^{3}He [27]. This requires the superfluid to be confined in a thin cavity of uniform thickness. At the heart of this predicted *stripe phase* is the stabilization of a hard domain wall, of thickness comparable to the superfluid coherence length, in superfluid ^{3}He-B under confinement in a slab geometry. These B-B domain walls were first classified in Ref. [28], and the analogy drawn with cosmic domain walls. Their stability in the bulk, and possible evidence for their observation is discussed in Ref. [29]. Under confinement the presence of the domain wall reduces surface pair breaking, and can result in a negative domain wall energy, leading to the formation of the stripe phase [27,30,31].

In superfluid ^{3}He the nuclear spins constitute the spin part of the pair wave function; thus nuclear magnetic resonance (NMR) is widely used to provide a direct fingerprint of the superfluid order parameter [4,5]. NMR has been predicted to distinguish clearly between the striped and translationally invariant states of the B phase [30,32].

To optimize the formation of stripes in this work we chose a slab geometry of height $D = 1.1\ \mu$m, where the B phase is stable down to zero pressure [33]. The stripe phase was originally predicted in the weak-coupling limit of Bardeen-Cooper-Schrieffer theory [27], while the strong-coupling corrections to this theory in general favor the A phase and suppress the stability of stripes [30]. At present the strong coupling effects are not fully understood theoretically, leaving the stability of the stripe phase an open question [30,33]. We performed the experiment at low pressure to minimize the strong-coupling effects.

Here we show that under our experimental conditions the stripe phase is clearly ruled out. However, there is NMR evidence for a spatially modulated superfluid of two-dimensional morphology, similar to states discussed in Ref. [11]; we term this *polka dot*.

The 3×3 matrix order parameter of a p-wave superfluid ^{3}He allows for multiple superfluid phases with different broken symmetries and topological invariants [4,5]. In the bulk, at low pressure and magnetic field the stable state is the quasi-isotropic B phase with order parameter matrix $\boldsymbol{A} = e^{i\phi}\boldsymbol{R}\Delta$, where Δ is the energy gap, isotropic in the momentum space, ϕ is the superfluid phase, and $\boldsymbol{R} = \boldsymbol{R}(\hat{\mathbf{n}}, \theta)$ is the matrix of the relative spin-orbit rotation, parametrized by angle θ and axis $\hat{\mathbf{n}}$. This quasi-isotropic phase is relatively easily distorted by magnetic field or flow. Under confinement the distortion is strong and spatially inhomogeneous, induced by surface pair breaking. In a slab normal to the z axis, the order parameter is predicted to take the form

$$\boldsymbol{A}(z) = e^{i\phi}\boldsymbol{R}\begin{pmatrix} \Delta_\parallel(z) & & \\ & \Delta_\parallel(z) & \\ & & \Delta_\perp(z) \end{pmatrix}, \qquad (1)$$

with $0 \le \Delta_\perp < \Delta_\parallel$ due to stronger surface pair breaking of Cooper pairs with orbital momentum parallel to the slab surface [34]. This distortion is named *planar* after the planar phase, in which $\Delta_\perp = 0$ [5].

The order parameter Eq. (1) has a large manifold of orientations, determined by ϕ, $\hat{\mathbf{n}}$, and θ, allowing domain walls between regions of different orientations [28,29]. Domain walls where $\Delta_\perp$ changes sign, shown in Fig. 1, are predicted to have negative surface energy in the B phase confined in a thin slab, close to the A-B transition [27,35]. As a consequence the slab of ^{3}He-B would spontaneously break into domains, until the domain walls get close enough that their mutual repulsion becomes significant. This is predicted to result in the periodic stripe phase with a typical domain size W of order D [27,30,31]. Phases with spontaneously broken translational invariance are also

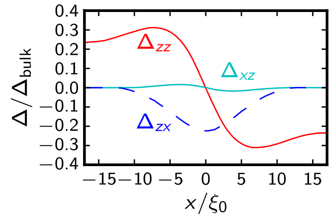

FIG. 1. Domain wall at the heart of the stripe phase in ^{3}He-B [27]. Shown here are the elements of the energy gap matrix Δ, such that $\boldsymbol{A} = e^{i\phi}\boldsymbol{R}\Delta$. When the domain wall is absent Δ is diagonal, see Eq. (1). Crossing the domain wall lying in the yz plane at $x = 0$, Δ_{zz} changes sign, and off-diagonal elements Δ_{xz} and Δ_{zx} emerge, while Δ_{xx} and Δ_{yy} (not shown) remain close to $\Delta_\parallel$. The gap amplitudes were calculated $z = 2.5\xi_0$ away from one of the surfaces in a $D = 10\xi_0$ thick slab at $T = 0.5T_c^{\rm bulk}$; ξ_0 is the Cooper pair diameter, $\Delta_{\rm bulk}$ is the bulk B phase gap.

predicted to stabilize in ^{3}He confined to narrow pores [36,37] and in films of d-wave superconductors [38].

In this experiment we performed pulsed NMR studies on a slab of ^{3}He confined in a $D = 1144 \pm 7$ nm thick silicon-glass microfluidic cavity, in a field of 31 mT perpendicular to the slab (corresponding to ^{3}He Larmor frequency $f_{\rm L} = 1.02$ MHz), using the setup described in Refs. [39,40]. The measurements were performed at low pressure $P = 0.03$ bar, where the bulk superfluid transition temperature $T_c^{\rm bulk} = 0.93$ mK, and close to specular scattering, achieved by preplating the cell walls with a 64 μmol/m^2 (∼5 atomic layers) ^{4}He film.

We first mapped the phase diagram with small tipping angle ($\beta = 4°$) NMR pulses, Fig. 2(a). The A-B transition was observed at $T_{AB} = 0.7T_c^{\rm bulk}$ in agreement with torsional oscillator measurements, with a 1.08 μm cavity [33]. As we previously observed in the 0.7 μm cavity, the B phase nucleated stochastically in two spin-orbit orientations with distinct NMR signatures: stable B_+ and metastable B_- [32,39].

The magnitudes of the frequency shifts of translationally invariant B_+ and B_-, Δf_+ and Δf_-, are determined by averages of the gap structure across the cavity [32]: $\langle\Delta_\parallel^2\rangle$, $\langle\Delta_\parallel\Delta_\perp\rangle$ and $\langle\Delta_\perp^2\rangle$. In case of the putative spatially modulated phase, the averaging is also performed in the plane of the slab. This procedure is valid when the width of the stripes W is smaller than the dipole length $\xi_D \approx 10\ \mu$m [32], a condition predicted to hold for this cavity ($W \approx D\sqrt{3} \ll \xi_D$), except very close to the stripe-to-B transition [30]. In the stripe phase $\langle\Delta_\parallel\Delta_\perp\rangle = 0$ due to $\Delta_\perp$ having opposite sign in the adjacent domains [32]. This has clear signatures in the NMR response, as a function of tipping angle β.

We define the dimensionless gap distortion parameters

$$\bar{q} = \langle\Delta_\parallel\Delta_\perp\rangle/\langle\Delta_\parallel^2\rangle, \qquad \bar{Q} = \sqrt{\langle\Delta_\perp^2\rangle/\langle\Delta_\parallel^2\rangle}. \qquad (2)$$

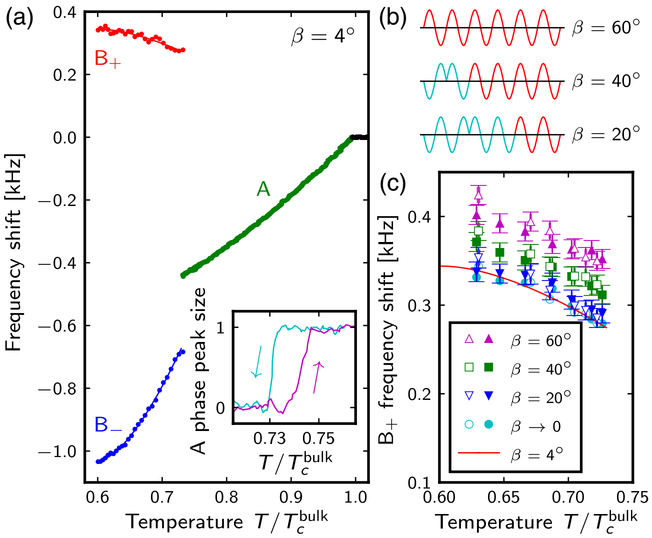

FIG. 2. NMR measurements on a $D = 1.1\ \mu$m slab of superfluid ^{3}He. (a) Signatures of the A and B phases observed with small tipping pulses. At the second-order normal-superfluid transition a negative frequency shift develops as the slab enters the A phase with the dipole-unlocked orientation. On further cooling a first-order phase transition into the B phase with a planar distortion occurs, where two spin-orbit orientations B_+ and B_- are observed. Inset: Sharp A-B transition with small hysteresis. (b) Technique for applying a set of pulses with different tipping angle β but equal heating: all pulses coincide in length and amplitude; β is reduced by applying the initial section of the pulse with a 180° phase shift, which cancels out a similar section that follows (both light blue), so only the remainder of the pulse (red) tips the spins. (c) Initial frequency shifts in B_+ after such pulses yield $\partial\Delta f_+/\partial\cos\beta$ and $\Delta f_+(\beta\to 0)$. Good agreement between $\Delta f_+(\beta\to 0)$ obtained here and $\Delta f_+(4°)$, smoothed from (a), indicates that the heating due to the 20°–60° pulses is negligible. Open (filled) symbols show data taken on stepwise warm-ups after fast (slow) cooldown from the A phase.

The tipping angle dependence of the frequency shift of B_+, below the so called "magic angle," $\beta^* > 104°$, scaled by the small-tipping-angle shift of B_-, is given by [32]

$$\frac{\Delta f_+(\beta\to 0)}{\Delta f_-(\beta\to 0)} = \frac{2\bar{Q}^2 - \bar{q}^2 - 1}{1 + 2\bar{Q}^2}, \tag{3a}$$

$$\frac{\partial\Delta f_+(\beta)/\partial\cos\beta}{\Delta f_-(\beta\to 0)} = \frac{2\bar{Q}^2 - 2\bar{q}^2}{1 + 2\bar{Q}^2}, \tag{3b}$$

where β is the tip angle. We further note that $\Delta f_-(\beta)$ does not depend on $\bar{q}$; the magic angle at which there is a kink in $\Delta f_+(\beta)$ is given by $\beta^* = \arccos(\bar{q} - 2)/(2\bar{q} + 2)$ [32]. Thus there is no magic angle expected for the stripe phase, for which $\bar{q} = 0$.

Application of large tipping pulses in our setup results in rapid heating of the confined helium via an unidentified mechanism, that previously restricted measurements of the planar distortion to temperatures well below T_{AB} [32,40]. Here we focus on moderate pulses, $\beta \lesssim 60°$, that allow us to probe the temperature dependence of the distortion parameters up to T_{AB}, according to Eq. (3). In order to measure the tipping-angle dependence of the frequency shift at constant temperature, we developed a scheme for applying pulses with different β while inducing identical heating, shown in Fig. 2(b). Triplets of such pulses with $\beta = 20°$ to 60° were applied to B_+ during stepwise warm-ups after a fast (at approx. 40 μK/ min rate) and slow (4 μK/ min) cooldown through the A-B transition. We inferred $\partial\Delta f_+/\partial\cos\beta$ and $\Delta f_+(\beta\to 0)$ from the data shown in Fig. 2(c) and confirmed the heating effects to be negligible for the chosen pulses. Combining with $\Delta f_-(4°)$ at the same temperature, Fig. 2(a), we determine the planar distortion parameters $\bar{q}$ and $\bar{q}$ through Eq. (3), shown in Fig. 3.

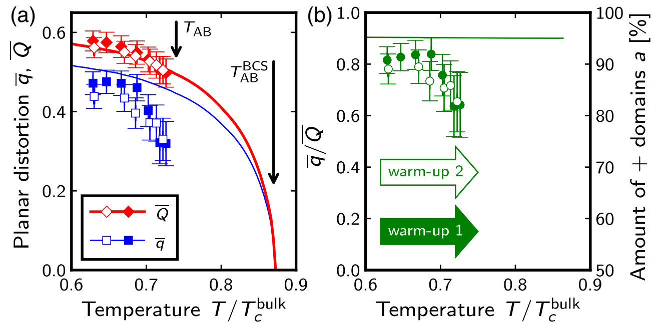

FIG. 3. Temperature dependence of planar distortion parameters $\bar{q}$, $\bar{Q}$ (a) and their ratio (b) inferred from NMR measurements, Fig. 2. Solid lines show weak-coupling calculations for the translationally invariant B phase [44]. In the absence of strong coupling the temperature of the A-B transition T_{AB}^{BCS} is higher than T_{AB} observed experimentally. While $\bar{Q}$ is in agreement with the theory, $\bar{q}$ gets progressively reduced approaching T_{AB}. We interpret this in terms of development of domains with opposite sign of $\Delta_\perp$ on warming. The right-hand vertical axis in (b) estimates the fraction of the slab occupied by the majority domains, taken here to have positive $\Delta_\perp$ [45], under a qualitative assumption of steplike energy gap profile, Eq. (4). Any systematic difference between measurements taken while warming after a fast and a slow cooldown through A-B transition (open/filled symbols) is small.

In the above analysis the off-diagonal elements of the gap matrix near domain walls (see Fig. 1) have been neglected. Incorporating the detailed gap structure at the domain walls into the NMR model leaves the signature of the stripe phase, $\bar{q} = 0$, $\bar{Q} > 0$, virtually unchanged [30]. We can therefore conclude unambiguously that the stripe phase was not present in our experiment.

Nevertheless, while $\bar{Q}$ matches the weak-coupling calculations for the translationally-invariant B phase [44], $\bar{q}$ is found to be reduced, see Fig. 3. This contrasts with the good agreement between these calculations and similar measurements in a $D = 0.7\ \mu$m slab at higher pressure [32,40], ruling out strong coupling effects as the origin of

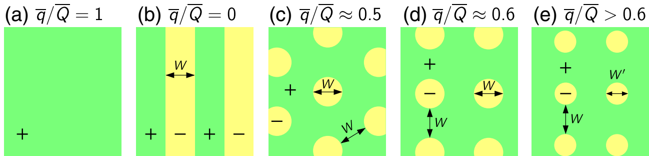

FIG. 4. Possible regular domain configurations in ^{3}He-B confined to a slab, view perpendicular to the slab plane. $+$ or $-$ indicates the sign of $\Delta_\perp$. (a) Translationally invariant B phase. (b) Predicted stripe phase. (c),(d) Proposed polka dot phase that is easier to nucleate than the stripe phase. The values of the gap distortion parameter $\bar{q}/\bar{Q}$ are derived under a simplified assumption of steplike domain walls, Eq. (4). Pinning of domain walls in the experimental cell may introduce disorder to these structures. All features in (c) and (d) are taken to be of characteristic size similar to the pitch W of the stripe phase. (e) A variant of (d) in which dot diameter W' is smaller than dot separation W.

this discrepancy. We therefore consider domain structures in which the amount a and $1-a$ of domains with positive and negative $\Delta_\perp$ is unequal [45]. For a qualitative estimate we assume that the domain walls are steplike and ignore gap variation across the slab, $\Delta_\parallel = \text{const}$, $|\Delta_\perp| = \text{const}$. Then

$$\bar{Q} = \frac{|\Delta_\perp|}{\Delta_\parallel}, \quad \bar{q} = (2a-1)\frac{|\Delta_\perp|}{\Delta_\parallel}, \quad \frac{\bar{q}}{\bar{Q}} = 2a-1, \tag{4}$$

demonstrating that while $\bar{q}$ is sensitive to the presence of domains, to the first approximation $\bar{Q}$ is not, in agreement with our observations. The gradual variation of $\Delta_\parallel$, $\Delta_\perp$ and the emergence of the off-diagonal gap matrix elements inside the domain walls would lead to corrections to this model that should be taken into account in future theoretical work.

Our measurement $\bar{q}/\bar{Q} = 0.6 \pm 0.1$ near T_{AB} suggests a $+/-$ domain proportion of 4:1. A likely scenario for an imbalance of the domains is a two-dimensional structure. Within possible regular morphologies, Fig. 4, this imbalance corresponds to a *polka dot phase* with hexagonal or square symmetry, Figs. 4(c) and 4(d). Such structures have been suggested theoretically [27], but the detailed analysis of their energetic stability has not been carried out. A preliminary Ginzburg-Landau study finds the square lattice of dots, Fig. 4(d), to be locally stable, with free energy only slightly higher than that of the stripe phase [46]. Further theoretical work is required to understand the stability of various modulated states in the presence of strong coupling effects.

Even if less energetically favorable than stripes, the dots may arise because of a lower energy barrier for flipping the sign of $\Delta_\perp$ in a microscopic dot, compared with a stripe, that is macroscopic in one dimension. A lattice of dots would form if the neighboring dots nucleate close enough to prevent them from growing beyond a typical size W before getting within W of the others.

Our experimental protocol is first to cool deep into the B phase, in order to destabilize the domain walls, and then to take data on warming. The key observation of the decrease in $\bar{q}/\bar{Q}$ with increasing temperature is consistent with the formation of negative-energy domain walls in the B phase approaching the transition into the A phase, as predicted theoretically. The observation of a single NMR line implies that the domain size is shorter than ξ_D. The measured temperature dependence of $\bar{q}/\bar{Q}$ can be explained by allowing the separation between dots W and their diameter W' to be unequal, see Fig. 4(e). Pinning of the domain walls by scratches on the cavity walls [47] may play a role in restricting W', and introduce disorder into the domain morphology. Improved cavities have been developed for future experiments [48].

As an alternative scenario, we now consider metastable domain walls with positive energy. Defects are known to form at the A-B transition either due to inhomogeneous nucleation [49,50] or as relics [51] of defects, present in the A phase at the start of the transition [52,53]. These may include the domain walls where $\Delta_\perp$ changes sign [29,51,54,55], which, if produced at unusually high density, would result in a reduced $\bar{q}/\bar{Q}$ ratio; however this ratio would remain constant if the defects are pinned or increase with time as they decay, contrary to our observation. This does not rule out sparse positive-energy defects with typical separation larger than ξ_D, giving rise to small satellite NMR signals, specific to each type of defect [51,53,56,57]. Detection of such signals is beyond the scope of this work. Within errors our observations are independent of the rate of cooling through the A-B transition, Fig. 3. This supports our proposal that defects produced at this transition do not play a major role in the formation of domains on the micron scale. A systematic study of the influence of the cooling rate will be the subject of future work.

In conclusion our NMR study of superfluid ^{3}He confined in a 1.1 μm cavity in the vicinity of the A-B transition has found neither the predicted stripe phase, nor the translationally invariant planar-distorted B phase. This leads us to propose a superfluid phase with two-dimensional spatial modulation, in a form of a regular or disordered array of island domains, driven by the negative energy of domain walls under confinement. Further systematic studies of the nucleation of this phase, to determine the equilibrium morphology, as well as its stability as a function of pressure, predicted to be influenced by strong coupling effects, are both desirable. Superfluid ^{3}He under confinement appears to provide a clean model system for spatially modulated superconductivity or superfluidity, long sought in a wide variety of physical systems.

We thank B. R. Ilic for help with microfluidic chamber fabrication and design methodology; A. B. Vorontsov and

J. A. Sauls for sharing calculations of the gap profile of confined ^{3}He; T. Kawakami and T. Mizushima for a stimulating discussion and for sharing their preliminary result on the stability of the polka dot phase. This work was supported by EPSRC Grants No. EP/J022004/1 and No. EP/R04533X/1; NSF Grants No. DMR-1202991 and No. DMR-1708341, and the European Microkelvin Platform.

[*]l.v.levitin@rhul.ac.uk
[†]Present address: Institute for Quantum Computing, University of Waterloo, Waterloo, Ontario N2L 3G1, Canada.
[‡]Present address: Imperial College London, London SW7 2AZ, United Kingdom.
[§]Present address: Corning Incorporated, USA.
[∥]Present address: Vantage Power Ltd, London UB6 0FD, United Kingdom.

[1] J. Bardeen, L. N. Cooper, and J. R. Schrieffer, Phys. Rev. **108**, 1175 (1957).
[2] L. N. Cooper, *BCS: 50 Years* (World Scientific, Singapore, 2011).
[3] G. R. Stewart, Adv. Phys. **66**, 75 (2017).
[4] A. J. Leggett, Rev. Mod. Phys. **47**, 331 (1975).
[5] D. Vollhardt and P. Wolfle, *The Superfluid Phases of* ^{3}*He* (Taylor & Francis, London, 1990).
[6] S. Giorgini, L. P. Pitaevskii, and S. Stringari, Rev. Mod. Phys. **80**, 1215 (2008).
[7] A. B. Migdal, Nucl. Phys. **13**, 655 (1959).
[8] A. A. Abrikosov, Sov. Phys. JETP **5**, 1174 (1957).
[9] A. I. Larkin and Yu. N. Ovchinnikov, Sov. Phys. JETP **20**, 762 (1965).
[10] P. Fulde and R. A. Ferrell, Phys. Rev. **135**, A550 (1964).
[11] Y. Matsuda and H. Shimahara, J. Phys. Soc. Jpn. **76**, 051005 (2007).
[12] J. Wosnitza, Ann. Phys. (Berlin) **530**, 1700282 (2018).
[13] H. Mayaffre, S. Krämer, M. Horvatić, C. Berthier, K. Miyagawa, K. Kanoda, and V. F. Mitrović, Nat. Phys. **10**, 928 (2014).
[14] C. C. Agosta, N. A. Fortune, S. T. Hannahs, S. Gu, L. Liang, J.-H. Park, and J. A. Schleuter, Phys. Rev. Lett. **118**, 267001 (2017).
[15] R. Beyer, B. Bergk, S. Yasin, J. A. Schlueter, and J. Wosnitza, Phys. Rev. Lett. **109**, 027003 (2012).
[16] G. Koutroulakis, H. Kühne, J. A. Schlueter, J. Wosnitza, and S. E. Brown, Phys. Rev. Lett. **116**, 067003 (2016).
[17] Sh. Kitagawa, G. Nakamine, K. Ishida, H. S. Jeevan, C. Geibel, and F. Steglich, Phys. Rev. Lett. **121**, 157004 (2018).
[18] A. Bianchi, R. Movshovich, C. Capan, P. G. Pagliuso, and J. L. Sarrao, Phys. Rev. Lett. **91**, 187004 (2003).
[19] G. Koutroulakis, M. D. Stewart, Jr., V. F. Mitrović, M. Horvatić, C. Berthier, G. Lapertot, and J. Flouquet, Phys. Rev. Lett. **104**, 087001 (2010).
[20] D. Y. Kim, S.-Z. Lin, F. Weickert, M. Kenzelmann, E. D. Bauer, F. Ronning, J. D. Thompson, and R. Movshovich, Phys. Rev. X **6**, 041059 (2016).
[21] D. Y. Kim, S.-Z. Lin, F. Weickert, E. D. Bauer, F. Ronning, J. D. Thompson, and R. Movshovich, Phys. Rev. Lett. **118**, 197001 (2017).
[22] M. H. Hamidian, S. D. Edkins, S. H. Joo, A. Kostin, H. Eisaki, S. Uchida, M. J. Lawler, E.-A. Kim, A. P. Mackenzie, K. Fujita, J. Lee, and J. C. Séamus Davis, Nature (London) **532**, 343 (2016).
[23] M. W. Zwierlein, A. Schirotzek, C. H. Schunck, and W. Ketterle, Science **311**, 492 (2006).
[24] M. C. Revelle, J. A. Fry, B. A. Olsen, and R. G. Hulet, Phys. Rev. Lett. **117**, 235301 (2016).
[25] R. Casalbuoni and G. Nardulli, Rev. Mod. Phys. **76**, 263 (2004).
[26] S. Dutta and E. J. Mueller, Phys. Rev. A **96**, 023612 (2017).
[27] A. B. Vorontsov and J. A. Sauls, Phys. Rev. Lett. **98**, 045301 (2007); J. Low Temp. Phys. **138**, 283 (2005).
[28] M. M. Salomaa and G. E. Volovik, Phys. Rev. B **37**, 9298 (1988).
[29] M. Silveri, T. Turunen, and E. Thuneberg, Phys. Rev. B **90**, 184513 (2014).
[30] J. J. Wiman and J. A. Sauls, J. Low Temp. Phys. **184**, 1054 (2016).
[31] K. Aoyama, J. Phys. Soc. Jpn. **85**, 094604 (2016).
[32] L. V. Levitin, R. G. Bennett, E. V. Surovtsev, J. M. Parpia, B. Cowan, A. J. Casey, and J. Saunders, Phys. Rev. Lett. **111**, 235304 (2013).
[33] N. Zhelev, T. S. Abhilash, E. N. Smith, R. G. Bennett, X. Rojas, L. Levitin, J. Saunders, and J. M. Parpia, Nat. Commun. **8**, 15963 (2017).
[34] Y. Nagato and K. Nagai, Physica (Amsterdam) **284B-288B**, 269 (2000).
[35] Note that the state with $\Delta_\perp < 0$ on the right of the domain wall in Fig. 1 can be written in the canonical form Eq. (1) with $\Delta_\perp > 0$ using a π phase shift and a combined rotation $\boldsymbol{R}(\hat{\mathbf{n}}', \theta') = \boldsymbol{R}(\hat{\mathbf{n}}, \theta)\boldsymbol{R}(\hat{\mathbf{z}}, \pi)$:

$$
\begin{aligned}
& e^{i\phi}\boldsymbol{R}(\hat{\mathbf{n}}, \theta)\begin{pmatrix} \Delta_\parallel & & \\ & \Delta_\parallel & \\ & & -\Delta_\perp \end{pmatrix} \\
&= -e^{i\phi}\boldsymbol{R}(\hat{\mathbf{n}}, \theta)\begin{pmatrix} -\Delta_\parallel & & \\ & -\Delta_\parallel & \\ & & \Delta_\perp \end{pmatrix} \\
&= e^{i(\phi+\pi)}\boldsymbol{R}(\hat{\mathbf{n}}, \theta)\boldsymbol{R}(\hat{\mathbf{z}}, \pi)\begin{pmatrix} \Delta_\parallel & & \\ & \Delta_\parallel & \\ & & \Delta_\perp \end{pmatrix}.
\end{aligned}
$$

[36] K. Aoyama, Phys. Rev. B **89**, 140502R (2014).
[37] J. J. Wiman and J. A. Sauls, Phys. Rev. Lett. **121**, 045301 (2018).
[38] A. B. Vorontsov, Phys. Rev. Lett. **102**, 177001 (2009).
[39] L. V. Levitin, R. G. Bennett, A. Casey, B. Cowan, J. Saunders, D. Drung, Th. Schurig, and J. M. Parpia, Science **340**, 841 (2013).
[40] See Supplemental Material at http://link.aps.org/supplemental/10.1103/PhysRevLett.122.085301 for details of the experimental setup, NMR, thermometry, comparison of the measured $\bar{q}$ and $\bar{Q}$ to Ref. [32], and qualitative

comparison of domain configurations. This includes Refs. [41–43].

[41] L. V. Levitin, R. G. Bennett, A. Casey, B. Cowan, J. Saunders, D. Drung, Th. Schurig, J. M. Parpia, B. Ilic, and N. Zhelev, J. Low Temp. Phys. **175**, 667 (2014).

[42] V. Dotsenko and N. Mulders, J. Low Temp. Phys. **134**, 443 (2004).

[43] P. J. Heikkinen, A. Casey, L. V. Levitin, X. Rojas, A. Vorontsov, N. Zhelev, J. M. Parpia, and J. Saunders (to be published).

[44] A. B. Vorontsov and J. A. Sauls, Phys. Rev. B **68**, 064508 (2003) and private communication.

[45] Since the sign of $\Delta_\perp$ can be flipped throughout the sample with a uniform transformation [35], we only need to consider the case of $\Delta_\perp$ being positive in the larger part of the slab, $a \geq 0.5$, so $\bar{q} \geq 0$, as required in Eq. (3) [32].

[46] T. Kawakami and T. Mizushima (private communication).

[47] Analogous to weak pinning of the *A*-*B* boundary observed in the similarly fabricated $D = 0.7$ μm cavity [39].

[48] N. Zhelev, T. S. Abhilash, R. G. Bennett, E. N. Smith, B. Ilic, J. M. Parpia, L. V. Levitin, X. Rojas, A. Casey, and J. Saunders, Rev. Sci. Instrum. **89**, 073902 (2018).

[49] D. I. Bradley, S. N. Fisher, A. M. Guénault, R. P. Haley, J. Kopu, H. Martin, G. R. Pickett, J. E. Roberts, and V. Tsepelin, Nat. Phys. **4**, 46 (2008).

[50] P. J. Heikkinen, S. Autti, V. B. Eltsov, R. P. Haley, and V. V. Zavjalov, J. Low Temp. Phys. **175**, 681 (2014).

[51] J. T. Mäkinen, V. V. Dmitriev, J. Nissinen, J. Rysti, G. E. Volovik, A. N. Yudin, K. Zhang, and V. B. Eltsov, Nat. Commun. **10**, 237 (2019).

[52] P. M. Walmsley and A. I. Golov, Phys. Rev. Lett. **109**, 215301 (2012).

[53] J. Kasai, Y. Okamoto, K. Nishioka, T. Takagi, and Y. Sasaki, Phys. Rev. Lett. **120**, 205301 (2018).

[54] Yu. Mukharsky, O. Avenel, and E. Varoquaux, Phys. Rev. Lett. **92**, 210402 (2004).

[55] C. B. Winkelmann, J. Elbs, Yu. M. Bunkov, and H. Godfrin, Phys. Rev. Lett. **96**, 205301 (2006).

[56] V. B. Eltsov, R. Blaauwgeers, N. B. Kopnin, M. Krusius, J. J. Ruohio, R. Schanen, and E. V. Thuneberg, Phys. Rev. Lett. **88**, 065301 (2002).

[57] S. Autti, V. V. Dmitriev, J. T. Mäkinen, A. A. Soldatov, G. E. Volovik, A. N. Yudin, V. V. Zavjalov, and V. B. Eltsov, Phys. Rev. Lett. **117**, 255301 (2016).